



From electromagnetic bandgap to left-handed metamaterials: modelling and applications^{*}

HAO Yang (郝 阳)

(The Department of Electronic Engineering, Queen Mary College, University of London, London, UK)

E-mail: y.hao@elec.qmul.ac.uk

Received Oct. 23, 2005; revision accepted Nov. 15, 2005

Abstract: In this paper, numerical modelling of left-handed materials (LHMs) is presented using in-house and commercial software packages. Approaches used include the finite-difference time-domain (FDTD) method, finite element method (FEM) and method of moments (MoMs). Numerical simulation includes verification of negative refraction and “perfect lenses” construction, investigation of evanescent wave behaviour in layered LHMs, reversed Snell’s Law in electromagnetic band gap (EBG)-like structures and construction of LHMs using modified split ring resonators (SRRs). Numerical results were verified to be in good agreement with theory. At the end of this paper, potential applications of LHMs in microwave engineering are discussed.

Key words: Numerical modelling, Electromagnetic crystals, Bandgap, Left-handed materials (LHMs)

doi: 10.1631/jzus.2006.A0034

Document code: A

CLC number: O441; TN204

INTRODUCTION

Electromagnetic crystal structures (ECSs) offer the opportunity to control and manipulate electromagnetic wave propagation as a result of their being formed from small-scale periodic geometric structures. This detailed microscopic configuration can be designed to cause the material (macroscopically) to exhibit either effective permittivity or permeability that is negative over a finite frequency range. This modifies the dispersion relation of electromagnetic waves and a band structure with a bandgap occurs in the case of electromagnetic band gap (EBG) structures (also called photonic band gap (PBG) structures). Such materials offer pass and stop bands to electromagnetic waves in the same way semiconductors offer these properties to electrons. Its application to antennas and RF passive components includes the suppression of surface waves, the construction of perfect magnetic conducting (PMC)

planes and antenna gain enhancement. Highlights of this work at Queen Mary College, University of London include characterization and application of anisotropic properties in EBG (Hao and Parini, 2002); antenna beam shaping using Fabry-Perot like EBG cavity (Zhao *et al.*, 2005); mobile antenna efficiency improvement using embedded uniplanar-compact (EUC) EBG structures (Hao *et al.*, 2004; Hao and Parini, 2003).

Left-handed materials (LHMs) are man-made engineering composites that, over a certain frequency band, exhibit electric permittivity and magnetic permeability which are both negative. This was theoretically predicted by Veselago (1968), who showed that LHMs exhibit anti-parallel nature in electromagnetic wave propagation and Poynting vectors. This is in contrast to conventional materials that normally carry electromagnetic wave energy in the same direction as they propagate and adhere to the so-called right-hand rule. Exciting possible electrodynamic properties for LHMs, such as reverse Doppler shift, Cherenkov radiation and inverse Snell effect, were identified. However, Veselago’s idea was

^{*} Project supported by the Royal Society, the Engineering and Physics Science Research Council (EPSRC) and the Leverhulme Trust, UK

forgotten because of the non-availability of realisable materials at that time. Recently, Pendry *et al.*(1999) demonstrated that materials with an array of split ring resonators (SRRs) produce negative permeability over certain frequency bands. Combining a two-dimensional (2D) array of SRRs interspersed with a 2D array of wires, to give negative permittivity, Smith *et al.*(2000) demonstrated for the first time the practical existence of LHMs. Although the doubts raised by some researchers about the existence of LHM has been answered by Smith *et al.*(2000), many questions remain concerning the effectiveness (Garcia and Nieto-Vesperinas, 2002) and applications for LHMs. Current LHM realisations are formed from periodic structures, as are EBG and frequency selective structures (FSSs). This naturally leads one to question whether all EBGs can be capable of exhibiting negative refraction phenomenon and if so, what are the necessary conditions that have to be maintained.

In this paper, numerical modelling of LHMs is presented. Approaches used include finite-difference time-domain (FDTD), finite element method (FEM) and method of moments (MoMs). Numerical simulation includes verification of negative refraction and “perfect lenses” construction; investigation of evanescent wave behaviour in layered LHMs; reversed Snell’s Law in EBG-like LHMs and construction of LHMs using modified SRRs. Numerical results were verified to be in good agreement with theory. At the end of this paper, potential applications of LHMs in microwave engineering are discussed.

DISPERSIVE FDTD MODELLING

The FDTD method, one of the most popular numerical methods in computational electromagnetics, was put forward by Yee (1966) and refined by many researchers in recent years. Significant research topics in this area include conformal FDTD (Hao and Railton, 1998), dispersive FDTD (Lu *et al.*, 2004) absorbing boundary conditions (ABCs), etc. It is important that FDTD modelling of LHMs must rely on dispersive FDTD since simultaneous negative values of permittivity and permeability can be realized only when there is frequency dispersion (Veselago, 1968). This can be seen from the relation between energy density W and electrical field \mathbf{E} and magnetic field \mathbf{H} .

$$W = \varepsilon \mathbf{E}^2 / 2 + \mu \mathbf{H}^2 / 2. \quad (1)$$

If both ε and μ are negative in value, and are non-dispersive, the total energy would be negative in this case, which will break the normal law of energy. When there is frequency dispersion, Eq.(1) must be replaced by

$$W = \frac{1}{2} \left\{ \frac{\partial[\varepsilon(\omega)\omega]}{\partial\omega} \mathbf{E}^2 + \frac{\partial[\mu(\omega)\omega]}{\partial\omega} \mathbf{H}^2 \right\}. \quad (2)$$

In order for the energy density W given by Eq.(2) to be positive, it is required that ε and μ must satisfy constraints:

$$\frac{d[\varepsilon(\omega)\omega]}{d\omega} > 0, \quad (3)$$

$$\frac{d[\mu(\omega)\omega]}{d\omega} > 0. \quad (4)$$

Following this rule, ε and μ can be defined in isotropic, lossy and cold plasma medium models (Hao and Railton, 1998).

$$\varepsilon(\omega) = \varepsilon_0 \left[1 - \frac{\omega_{pe}^2}{\omega(\omega - j\nu_e)} \right], \quad (5)$$

$$\mu(\omega) = \mu_0 \left[1 - \frac{\omega_{pm}^2}{\omega(\omega - j\nu_m)} \right], \quad (6)$$

where ω_{pe} is the electronic plasma frequency, ω_{pm} is the magnetic plasma frequency. ν_e is electric collision frequency and ν_m is magnetic collision frequency. We only consider TM excitation in 2D dispersive FDTD simulation. From the equivalent TM set of E_z , H_x and H_y , combining the frequency-domain constitutive relationship, $\hat{\mathbf{D}} = \hat{\varepsilon} \hat{\mathbf{E}}$ and $\hat{\mathbf{B}} = \hat{\mu} \hat{\mathbf{H}}$, we rewrite Maxwell’s equations as follows:

$$\partial D_z / \partial t = \partial H_y / \partial x - \partial H_x / \partial y, \quad (7)$$

$$D_z = \varepsilon_0 \left[1 - \frac{\omega_{pe}^2}{\omega(\omega - j\nu_e)} \right] E_z, \quad (8)$$

$$\partial B_x / \partial t = -\partial E_z / \partial y, \quad (9)$$

$$B_x = \mu_0 \left[1 - \frac{\omega_{pm}^2}{\omega(\omega - j\nu_m)} \right] H_x, \quad (10)$$

$$\partial B_y / \partial t = \partial E_z / \partial x, \quad (11)$$

$$B_y = \mu_0 \left[1 - \frac{\omega_{\text{pm}}^2}{\omega(\omega - j\nu_m)} \right] H_y. \quad (12)$$

Since multiplications of $j\omega$ in the frequency domain are equivalent to time derivatives in the time domain, Eqs.(8), (10) and (12) can be modified into the following second-order differential equations:

$$\frac{\partial^2 D_z}{\partial t^2} + \nu_e \frac{\partial D_z}{\partial t} = \varepsilon_0 \frac{\partial^2 E_z}{\partial t^2} + \varepsilon_0 \nu_e \frac{\partial E_z}{\partial t} + \varepsilon_0 \omega_{\text{pe}}^2 E_z \quad (13)$$

$$\frac{\partial^2 B_x}{\partial t^2} + \nu_m \frac{\partial B_x}{\partial t} = \mu_0 \frac{\partial^2 H_x}{\partial t^2} + \mu_0 \nu_m \frac{\partial H_x}{\partial t} + \mu_0 \omega_{\text{pm}}^2 H_x \quad (14)$$

$$\frac{\partial^2 B_y}{\partial t^2} + \nu_m \frac{\partial B_y}{\partial t} = \mu_0 \frac{\partial^2 H_y}{\partial t^2} + \mu_0 \nu_m \frac{\partial H_y}{\partial t} + \mu_0 \omega_{\text{pm}}^2 H_y \quad (15)$$

Then Eqs.(7), (9) and (12) are discretised on the standard Yee's lattice, along with discretization of Eqs.(13)~(15) approximated by the second-order central differences, yielding a group of iteration equations, which can be used in the modelling of LHMs (Lu *et al.*, 2004).

“PERFECT LENS” FDTD SIMULATION

Veselago (1968) and Pendry (2000) show that LHMs focus light “perfectly” even when it is in the form of a parallel-sided slab, which is different from that of a conventional classic lens. This idea was verified by Ziolkowski and Heyman (2001) using FDTD technique, in which only far field imaging from LHM was presented, although the effect from surface wave loss was not tackled. Such effects will in fact degrade the ‘perfection’ of flat lens constructed by LHM, particularly when the near field imaging is studied. Feise *et al.*(2002) performed some calculations using the macroscopic Maxwell equations on the behaviour of evanescent waves in LHM. It was shown that a ‘vanishing transition layer’ between an LHM slab and free space can give the ideal case with perfect construction of a point source. Ramakrishna and Pendry (2002) were the first to reveal that a thin LHM slab can be used to enhance the amplitude of evanescent waves in near field imaging. Their idea was then further developed into a multilayer stack of

thin alternating layers of conventional active materials and lossy LHM which transports evanescent waves over large stack thickness at the frequency of visible light (Ramakrishna and Pendry, 2002; Shamonina *et al.*, 2001). The theoretical prediction was verified using negative-refractive-index transmission-line media (Grbic and Eleftheriades, 2003). Lu *et al.*(2004) attempted to show with modelling that evanescent wave losses can reduce the quality of the image when a source point is close to an LHM lens, and then attempted to show with modelling that alternately layered stacks of positive and negative dielectrics can be used to reduce surface wave losses.

More discussion on why such a structure seems to guide the evanescent wave, and on the nature and quality of the created image will be very interesting. The results will certainly help to validate the feasibility of using macroscopic ε and μ in LHM numerical modelling, which was questioned in (Feise *et al.*, 2002). Our view is that given sufficient resolution, dispersive FDTD can successfully predict evanescent wave effects on the quality of imaging from conventional single-layer LHM slab, and show how it guides evanescent waves in the multilayer structure at microwave frequencies.

In our simulation, a continuous-wave (CW) point source of E_z field at 30 GHz was used. Other parameters were set as

$$\omega_{\text{pe}} = \omega_{\text{pm}} = \sqrt{2}\omega_0, \quad \nu_e = \nu_m = 0.$$

At resonant frequency ω_0 ,

$$\varepsilon_r(\omega_0) = \mu_r(\omega_0) = -1.$$

It is known that planar antenna design uses a thin dielectric substrate to reduce surface wave loss. Ramakrishna and Pendry (2002) applied the idea in LHM for near-field imaging and revealed that a thin slab enhances the evanescent waves, which are usually decayed exponentially in amplitude in its propagation directions. Current studies on evanescent wave behavior in LHMs are largely based on analytical or the transfer matrix method (TMM) (Ramakrishna and Pendry, 2002). Regarding FDTD modelling, there is strong indication in (Feise *et al.*, 2002) that the use of macroscopic ε and μ may not be appropriate at the interface of the forward-wave and

backward wave materials, hence a transition layer which is much thinner than the free space wavelength is needed for ideal construction of a point source. Here we apply dispersive FDTD program for modelling evanescent wave behavior in a thin layer LHM slab, and show the feasibility of using macroscopic representation of ϵ and μ and the numerical accuracy against spatial discretization resolution in LHM FDTD modelling. Fig.1 presents FDTD simulation results showing near field image in a thin LHM slab with width of $\lambda/10$ and height of 3λ . The cell size in FDTD space was $\lambda/80$. It can be seen in Fig.1 that evanescent wave attenuates very rapidly at the left hand side of the slab, but is amplified within the thin slab before merging with a near image at the right hand side of the slab. Both object and image planes are marked in Fig.1. The condition for existence of this phenomenon is that refractive index $n=-1$ at the operating frequency to ensure exciting of plasmon modes. The result verified that evanescent wave propagation should satisfy the Maxwell's equations and can be numerically represented using FDTD, and that no additional layer is required in LHM modelling as suggested in (Feise *et al.*, 2002). Fig.2 shows how evanescent wave propagates without attenuation through layered LHMs structures using a dispersive FDTD approach.

HFSS MODELLING OF EBG-LIKE STRUCTURE FOR NEGATIVE REFRACTIONS

AnsoftTM HFSS is based on FEM and extremely efficient when modelling curved electromagnetic structures. However, as the software is not capable of

specifying dispersive permittivity and permeability in materials, it is impossible to apply it in the "perfect lens" modeling mentioned above. In our study, HFSS was used to verify negative refractions from EBG-like structures and proved to be very effective. Current LHM realisations are formed from periodic structures, as are EBG and FSSs. This naturally leads one to question whether all ECS can be capable of exhibiting negative refraction phenomenon and if so, what are the necessary conditions that have to be met. In (Luo *et al.*, 2003), all angle negative refractions were identified from metallic photonic crystals. Negative refraction is also observed from a metallic photonic structure at frequencies near the stop band (Parimi *et al.*, 2004). Hao *et al.* (2003) pointed out that spatial harmonics may affect the characterisation of LHMs and sometimes enhance negative refractions in EBG-like structures.

In the regime of microwave applications, it is not always true that the spacing of the periodic structure is much less than the operating wavelength. In most photonic band gap applications and backward wave radiating structures, we can see that the period is comparable to the operating wavelength and hence our study yields insight into how we can effectively predict negative refraction from such EBG-like structures. Our approach is to analyse the entire finite periodic structure as a cell so that the effects of spatial harmonics will be considered. The dispersion diagram can be obtained from calculated S parameters. A detailed procedure for finding out dispersion behaviour from S parameters is discussed in (Collin, 1966). In order to get negative refraction at a specific frequency, the propagation constant at that frequency point should be negative ($\beta < 0$) so that electromagnetic

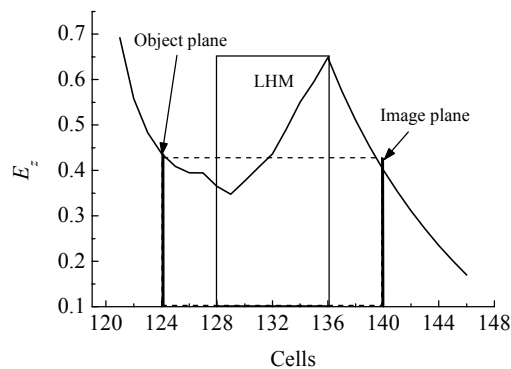


Fig.1 Demonstration of near field imaging simulated by dispersive FDTD: The ray diagram confirms reversing Snell's Law

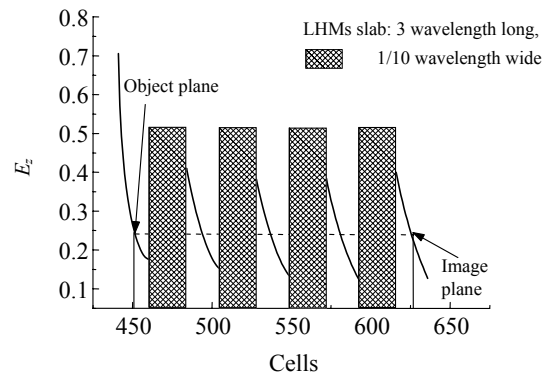


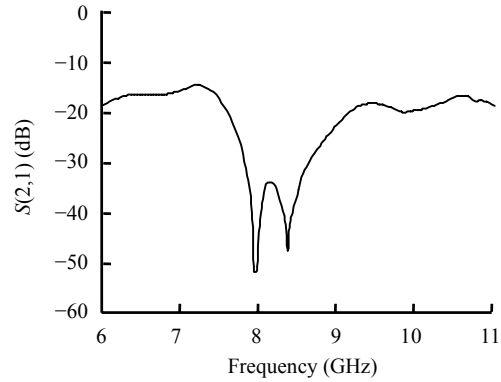
Fig.2 Dispersive FDTD simulation of near field intensity through multilayered LHMs structure with refractive index $n=-1$. Cell=wavelength/220

wave propagating in such a structure can have a negative phase velocity, and at the same time the propagating wave should also show a positive group velocity (positive slope in the dispersion diagram). Therefore the structure will exhibit negative refraction and backward radiation. Our analysis found that a periodic structure can give rise to negative refraction at some specific frequency which can be determined from the dispersion diagram obtained. Our simulation showed that when the number of elements in the structure increases, high order spatial harmonics are excited and the dispersion behaviour of the whole structure will change. In this paper, we assume that the loss of structure in the numerical analysis is very small and hence negligible.

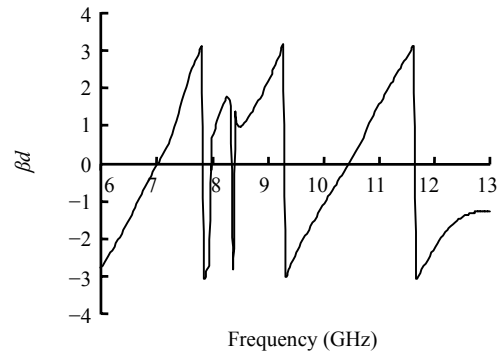
Firstly, we considered an EBG-like structure consisting of metallic wires of radius 0.63 cm and height 1.26 cm. We set the period of this structure as 1.46 cm and hence the radius is set to the period ratio $r/a=0.43$. The wires are arranged in prism shape with 12 elements in the base and vertical sides respectively. A focus beam obtained from a rectangular dielectric waveguide, with each side having the same length of 5 mm, was used as the incident field. When the wave is emitted from the structure, refraction should occur at the edge of the prism. The dispersion diagram obtained for the structure is shown in Fig.3b and the transmission coefficient $S(2,1)$ obtained for the structure is given in Fig.3a, in which a clear band gap can be seen at around 7.44~8.77 GHz. The dispersion diagram (Fig.3b) shows that there is positive refraction at 5.4 GHz and negative refraction at 5.7 GHz; these were validated by numerical simulation using AnsoftTM HFSS. We can see the wave-propagation direction turns to the positive side at 5.4 GHz and to the negative side at 5.7 GHz (Fig.4).

PLANAR LHMS MODELLING

Planar structures have advantages of easy fabrication, low profile and low costs. The structure presented in Fig.5 consists of SRRs and wires on a printed circuit board with ground plane (thickness 1.524 mm and $\epsilon_r=3$). This structure can be modeled ideally using Momentum from Agilent Technologies. We adopted a 2D structure consisting of 10×5 unit cells which are about $3.4 \text{ mm} \times 3.4 \text{ mm}$ each, with the length of the thin copper wires being about 20 mm.

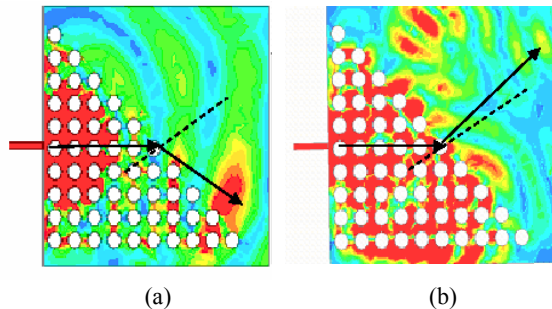


(a)



(b)

Fig.3 HFSS simulation results on an EBG-like structure. (a) Transmission coefficient; (b) Dispersion diagram



(a)

(b)

Fig.4 Field plot from HFSS simulation indicating both negative and positive refraction at different frequencies in a prism EBG-like structure. (a) Positive refraction at 2.9 GHz; (b) Negative refraction at 7.6 GHz

The width of metal strips in SRRs and metal wires was 0.25 mm; the gap between inner and outer rings was 0.38 mm. The period of SRRs was about 4.2 mm. Fig.6 shows that the transmission was increased due to the negative refractive index at frequency range 9~9.45 GHz where the dispersion curve shows negative phase velocity and positive group velocity (Fig.7a)

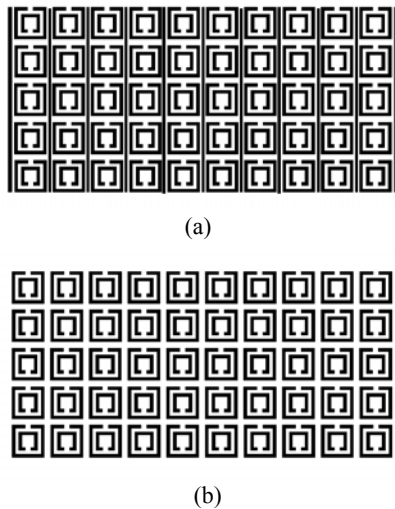


Fig.5 (a) SRRs with metal wires for LHMs structure; (b) SRRs only structure

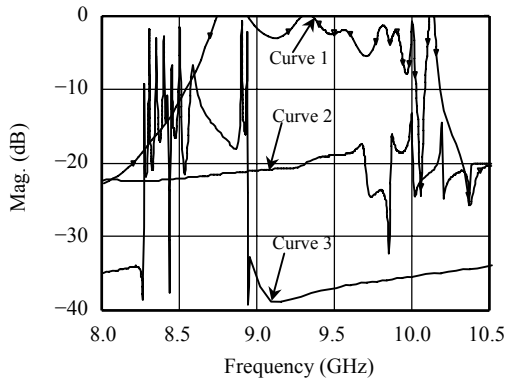
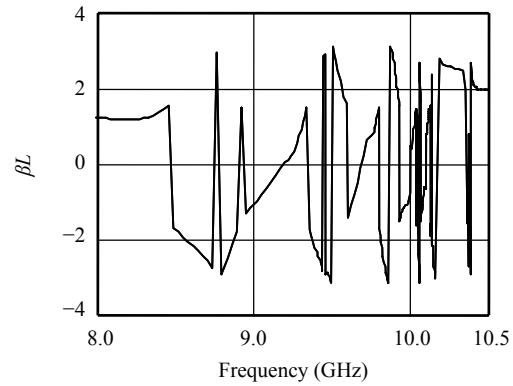
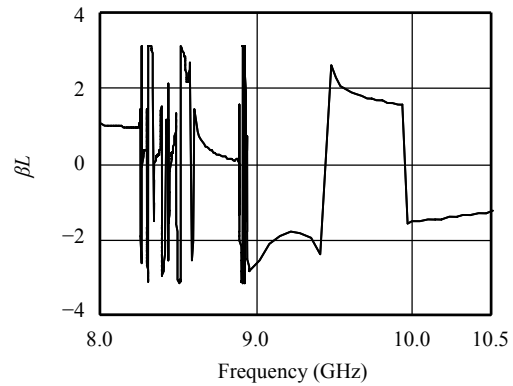


Fig.6 Transmissions comparison between SRRs with metal wires, SRRs only and wires only structures
Curve 1: metal wires; Curve 2: SRRs only structures;
Curve 3: wires only structures

for LHMs. For SRRs only structure (Fig.7b), it has plasma frequency of around 8.8 GHz but strong attenuation is shown at 9~9.45 GHz frequency band. Fig.7 shows that negative dispersion also occurs for SRRs only structure in some extremely narrow frequency bands from 8.3 GHz to 8.9 GHz. In our view, this is because in SRRs only structure, spatial harmonics contribution is more significant and gives rise to negative refraction for narrow frequency bands only. From the simulation we can notice that transmission of structure with SRR alone is enhanced by including wires. This can be explained by the fact that when wires are included, the effect of higher order spatial harmonics is reduced by decreasing d and hence increased λ_0/d value.



(a)



(b)

Fig.7 (a) Dispersion diagram for SRRs and wire structure; (b) Dispersion diagram for SRRs structure only

LHMS APPLICATIONS AND DISCUSSION

It is known that near field LHMs lenses may be used to see tiny structures like atoms since evanescent waves excited can be amplified and guided through layered structures. Apart from this, LHMs application in microwave and antenna engineering is not very clear. In our view, LHM may act as artificial PMC ground plane and may also be used for construction of TEM rectangular waveguides due to its property of inversed Snell's Law. Layered LHMs used for evanescent wave amplification also show no phase delay over a distance, which may be applied in broadband radar system design.

In conclusion, dispersive FDTD is a reliable tool that can be used to investigate the properties of LHMs, which are dispersive in nature, and is particularly critical as LHMs are currently not available in practice. Therefore, dispersive FDTD code can be used to predict novel applications which LHMs may bring

into electromagnetics, microwave and antenna engineering. Commercial software packages, such as HFSS and Momentum, have been used to simulate EBG-like structures and SRR-wire structures. Simulation results indicate that negative refraction may be observed from EBG-like structures and that spatial harmonics may narrow LHMs bandwidth. Experimental verification will be carried out in our future work.

ACKNOWLEDGEMENT

The work presented here was based on studies of Ms. Ling Lu, Mr. Sunil Sudhakaran, Mr. Daniel Nyberg and Prof. Haim Cory while they were at Queen Mary College, University of London. The author thanks Profs Peter Clarricoats, Clive Parini, Queen Mary College, London, for some useful discussions.

References

- Collin, R.E., 1966. Foundations for Microwave Engineering. Sec 8.9. McGraw-Hill Kogakusha Ltd.
- Garcia, N., Nieto-Vesperinas, M., 2002. Left-handed materials do not make a perfect lens. *Phys. Rev. Lett.*, **88**(20):207403. [doi:10.1103/PhysRevLett.88.207403]
- Gedney, S.D., 1996. An anisotropic perfectly matched layer-absorbing medium for the truncation of FDTD lattices. *IEEE Trans. Antenna and Propagation*, **44**(12): 1630-1639. [doi:10.1109/8.546249]
- Grbic, A., Eleftheriades, G.V., 2003. Growing evanescent waves in negative-refractive-index transmission-line media. *Applied Physics Letters*, **82**(12):1815-1817. [doi:10.1063/1.1561167]
- Hao, Y., Parini, C.G., 2002. Isolation enhancement of anisotropic UC-PBG microstrip diplexer patch antenna. *IEEE Antennas and Wireless Propagation Letters*, **1**:135-137. [doi:10.1109/LAWP.2002.806757]
- Hao, Y., Parini, C.G., 2003. Microstrip antennas on various UC-PBG substrates. *IEICE Trans. on Electronics*, Special Issue on Microwave and Millimeter-wave Technology.
- Hao, Y., Railton, C.J., 1998. Analyzing electromagnetic structures with curved boundaries on Cartesian FDTD meshes. *IEEE Transactions on Microwave Theory & Techniques*, **46**(1):82-88. [doi:10.1109/22.654926]
- Hao, Y., Sudhakaran, S., Parini, C.G., 2003. Spatial Harmonics Effects on Characterisation of Left-Handed Metamaterials. Asia-Pacific Microwave Conference, Korea.
- Hao, Y., Alomainy, A., Parini, C.G., 2004. Antenna beam shaping from offset defects in UC-EBG cavities. *Microwave and Optical Technology Letters*, **43**(2):108-112. [doi:10.1002/mop.20391]
- Lu, L., Hao, Y., Parini, C.G., 2004. Dispersive FDTD characterization of no phase-delay radio transmission over layered left-handed meta-materials structure. *IEE Proceedings-Science Measurement and Technology*, **151**(6): 403-406. [doi:10.1049/ip-smt:20040948]
- Luo, C.Y., Johnson, S.G., Joannopolous, J.D., Pendry, J.B., 2003. Negative refraction without negative index in metallic photonic crystals. *Optics Express*, **11**(7):746-754.
- Feise, M.W., Bebelacqua, P.J., Schneider, J.B., 2002. Effects of surface waves on the behavior of perfect lenses. *Physical Review B*, **66**:035113. [doi:10.1103/PhysRevB.66.035113]
- Parimi, P.V., Lu, W.T., Vodo, P., Sokoloff, J., Sridhar, S., 2004. Negative refraction and left-handed electromagnetism in microwave photonic crystals. *Phys. Rev. Lett.*, **92**:127401. [doi:10.1103/PhysRevLett.92.127401]
- Pendry, J.B., 2000. Negative refraction makes a perfect lens. *Phys. Rev. Lett.*, **85**:3966. [doi:10.1103/PhysRevLett.85.3966]
- Pendry, J.B., Holden, A.J., Robbins, D.J., Stewart, W.J., 1999. Magnetism from conductors and enhanced nonlinear phenomena. *IEEE Transactions on Microwave Theory & Techniques*, **47**(11):2075-2084. [doi:10.1109/22.798002]
- Ramakrishna, S.A., Pendry, J.B., 2002. The asymmetric lossy near-perfect lens. *Journal of Modern Optics*, **49**(10): 1747-1762. [doi:10.1080/09500340110120950]
- Shamonina, E., Kalinin, V.A., Ringhofer, K.H., Solymar, L., 2001. Imaging, compression and Poynting vector streamlines for negative permittivity materials. *Electronics Letters*, **37**(20):1243-1244. [doi:10.1049/el:20010863]
- Smith, D.R., Padilla, W.J., Vier, D.C., Nemat-Nasser, S.C., Schultz, S., 2000. Composite media with simultaneously negative permeability and permittivity. *Phys. Rev. Lett.*, **84**:4184-4187. [doi:10.1103/PhysRevLett.84.4184]
- Sudhakaran, S., Hao, Y., Parini, C.G., 2004. An enhanced prediction of negative refraction from EBG-like structures. *Microwave and Optical Technology Letters*, **41**(4):258-261. [doi:10.1002/mop.20110]
- Sudhakaran, S., Hao, Y., Parini, C.G., 2005. Negative refraction phenomenon at multiple frequency bands from electromagnetic crystals. *Microwave and Optical Technology Letters*, **45**(6):465-469. [doi:10.1002/mop.20854]
- Veselago, V.G., 1968. The electrodynamics of substances with simultaneously negative values of ϵ and μ . *Soviet Physics Uspekhi*, **10**(4):509-514. [doi:10.1070/PU1968v010n04.ABEH003699]
- Yee, K.S., 1966. Numerical solution of initial boundary value problems involving Maxwell's equations in isotropic media. *IEEE Trans. Antennas Propagation*, **14**:302-307. [doi:10.1109/TAP.1966.1138693]
- Zhao, Y., Hao, Y., Parini, C.G., 2005. Radiation properties of PIFA on UC-EBG substrates. *Microwave and Optical Technology Letters*, **44**(1):21-24. [doi:10.1002/mop.20535]
- Ziolkowski, R.W., Heyman, E., 2001. Wave propagation in media having negative permittivity and permeability. *Phys. Rev. E*, **64**:056625. [doi:10.1103/PhysRevE.64.056625]